Available online at www.sciencedirect.com

ScienceDirect

Physics Procedia 66 (2015) 548 – 555

Physics Procedia

C 23rd Conference on Application of Accelerators in Research and Industry, CAARI 2014

Nano-Crystal Formation and Growth from High-Fluence Ion Implantation of Au, Ag or Cu in Silica

D.ILA[a]*, J.E.E. Baglin[b], and R.L. Zimmerman[a]

[a] *Chemistry and Physics, Fayetteville State University, Fayetteville NC 28301-4297, USA*
[b] *IBM Almaden Research Center, San Jose, CA 95120, USA*

Abstract

The linear and non-linear optical properties of silica may be tailored by the introduction of a random distribution of nanocrystallites of an immiscible metal within a near-surface region. The size, size distribution, and spatial distribution of these crystallites must be controllable in order to optimize the functional properties for device applications. In this paper, we present a novel fabrication technique that offers such control. Energetic metal ions are implanted in silica at room temperature. Subsequent heat treatment leads to diffusion of the implanted atoms, nucleation and growth of metal crystallites, and Ostwald ripening of the resulting clusters. We have observed the kinetics and effective activation energies describing the multiple processes involved, for the cases of Au, Ag or Cu implanted at MeV energies, at various fluences, and then annealed at fixed temperatures in the range 500°C-1000°C. Effective activation energies found for nanocrystal nucleation and growth at temperatures below 800°C (e.g. 64 meV for Ag) are replaced above this temperature range by much higher activation energies (e.g. 400 meV for Ag). We may attribute this to the depletion of un-attached mobile metal atoms (so that ripening of clusters will be limited by energy barriers for escape of such mobile atoms from small crystallites), and/or the annealing of implant-caused stress in the silica structure at high temperatures, that creates new channels for thermal diffusion of metal atoms within the silica host.

Selection and peer-review under responsibility of the Organizing Committee of CAARI 2014

Keywords: Optical properties silica; metal nanoparticles; nanocrystal; growth kinetics; activation energy .

* Corresponding author. Tel.: +1-256-651-9603; fax: +1-910-672-2110.
E-mail address: daryushila@aol.com, dila@uncfsu.edu

Selection and peer-review under responsibility of the Organizing Committee of CAARI 2014
doi:10.1016/j.phpro.2015.05.073

Introduction

In the past three decades, ion implantation has been used to introduce foreign atoms into pure silica in order to change linear and nonlinear optical properties in layers near the sample surface [1-11]. Historically, foreign atoms were introduced near the surface of a material by thermal diffusion. Recently, layered structures of metal atoms in an insulator host, useful for specific quantum devices and promising innovative thermoelectric materials, have been fabricated by co-deposition of multiple layers on an appropriate substrate, each layer having a controlled metal/host atomic ratio.

After introduction of atoms into a host for which they have no chemical affinity, (Au, Ag or Cu in silica, for example), nanoclusters may be formed by thermal or laser annealing. Alternatively, energy may be supplied by irradiation [5,6] of the sample by MeV ions that pass completely through the layers of interest. An attractive feature of co-deposition followed by post implantation bombardment by MeV ions [6] to form nanoclusters is that the change in the linear and nonlinear properties of an optical host material occurs in a well-defined spatial region, and thus, by employing a highly focused ion beam, point quantum confinement in 3D arrays of nanoclusters may be accomplished. Materials with completely new properties can thus be engineered, unlike materials generated by the classical technique of ion implantation followed by thermal annealing.

A full understanding of the thermal kinetics for formation and evolution of metal nanoclusters in insulator materials is necessary, in order to develop future effective processes for inducing nanocluster formation by introduction of energy in other forms, for example, post implantation ion bombardment. However, this paper reports experiments based on purely thermal annealing of pre-implanted material.

To further this understanding, we have revisited data from the presentations made by the authors in Il Ciocco, Italy in 1996, and at IBMM and MRS conferences in 1996. These data appeared in subsequent publications reporting the radius of nanocrystals of gold, silver and copper in silica [1, 2] after thermal annealing at various temperatures, each for a fixed time.

Individual samples were prepared with Au, Ag or Cu atoms introduced by MeV implantation at room temperature into Suprasil-300, a commercial product of Heraeus Amersil, Inc. with known low contamination of OH and metal impurities. Heat treatment of the pre-implanted samples was then performed Each pre-implanted sample was subjected to heat treatment for 1 hour at a specific temperature, in an ambient of 1% hydrogen and 99% nitrogen. Each sample was then analyzed at room temperature, using Rutherford Backscattering Spectrometry (RBS), Optical Absorption Photometry (OAP), and in some cases, TEM. RBS served to confirm that no significant change in the overall depth distribution of the metal-implanted layer had occurred. The OAP spectra enabled assessment of the average size of metal nanoparticles found, before and after heat treatment. The growth of such metal clusters was studied, with respect to its dependence on metal species, implant fluence, and temperature of the post-implant heat treatment T(°K). As we shall show, the Arrhenius plots of cluster size vs. 1/kT all displayed an abrupt change of slope in the region of 800°C, implying the onset of a new and dominant growth process for the higher temperature range, characterized by a much larger effective activation energy than that of the lower temperature cluster formation fed by diffusion of individual mobile metal atoms.

We assume that the low temperature regime represents a simple diffusion-limited process of nucleation and growth of metal nano-crystallites, resulting from thermal migration of metal atoms within the (irradiation damaged and stressed) silica host. The onset of the higher temperature regime might then be attributable to a change of density or void structure in the annealed host silica, thus changing the local metal-silica interface energy and diffusion pathways, [12] and facilitating the cluster growth (Ostwald ripening) process of the metal nano-clusters. Alternatively, the effect may indicate a change of kinetics for Ostwald ripening when the clusters reach a critical size. Such possibilities invite further detailed study, with a prospect of identifying useful process parameters for future fabrication of materials having tailored optical performance.

In this manuscript, we highlight the direct experimental evidence of the change in the mechanism of nucleation and growth of nanocrystals, by showing the abrupt changes that occur in the activation energy for the formation of nanocrystals by thermal annealing as the average cluster radius increases beyond about 1 to 3 nanometers.

In the following section, we review our previous experiments on which our present analysis of the kinetics of nanocluster evolution is based.

Experimental procedures

For these investigations, we used silica glass substrates, provided as Suprasil-300 by Heraeus Amersil. Suprasil-300 contains 150 ppm OH, 0.05 ppm of Ti, Na, Ca and Al and less than 0.01 ppm other metals. The 10 × 10 × 1.5 mm^3 samples were implanted with 2.0 MeV copper, 1.5 to 2.0 MeV silver, or 2.0 to 3.6 MeV gold ions (with projected ranges about 1-2 microns in silica), at current densities less than 2 $\mu A/cm^2$, the target holder being cooled to room temperature to avoid premature formation of metal clusters due to ion beam heating. Ion fluences were chosen to give a guest atom to silicon ratio between 1:100 and 1:10. This allowed us to avoid the threshold fluence for each implanted ion species for spontaneous cluster formation. TEM and optical absorption photometry were used to confirm that nanocrystals were not present in the implanted samples before our thermal annealing experiments.

The thermal treatments were conducted at temperatures between 500°C and 1200°C and were accomplished for several time periods between 0.5 h and several hours for each treatment temperature. After each heat treatment, an optical absorption spectrum at room temperature was acquired. Using these spectra, the RBS results, and SRIM simulations [13], we calculated the average radius of the metallic nanoclusters in each case. .

The determination of average nanocluster radius from the optical absorption band is described in our previous publications [1, 2, 5, 6, 9, 14]. The optical absorption method is not as precise as the results available by transmission electron microscopy (TEM), but the results obtained from the optical absorption band are statistically representative of changes in the a much larger volume of the nanoclusters at each heat treatment than if the sampling had been done by TEM [2, 5, 6, 14]. Briefly, the average radius of metal spheres r, small compared with the wavelength of light, can be calculated from the resonance optical absorption spectrum [15,16] according to the equation

$$r = V_f / \Delta\omega \,, \tag{1}$$

where V_f is the Fermi velocity of electrons in the metal and $\Delta\omega$ is the full width at half maximum of the absorption band due to the plasmon resonance in the small metal particles. The frequency interval $\Delta\omega$ is related to the corresponding wavelength interval $\Delta\lambda$ on the OAP graphs.

During sample preparation, we observed that the higher the atomic number and fluence of the implanted metal ions, the more the damage and modification of the optical properties [17,18] of the silica glass, as observed by absorption spectrometry after implantation but before thermal treatment. Our previous research [1, 2, 5, 6, 9, and 14] has shown that low temperature treatment of the implanted samples reduces strains and charge imbalances caused by implantation of the metal species. Except for the effects attributable to the formation of metal nanoclusters, such spurious effects found in the as-implanted samples disappear with heat treatments above 500°C-700°C.

We used ion fluences from 2×10^{16} to 2×10^{17} ion/cm^2 for each implanted species to determine (and avoid) the higher fluences that would trigger spontaneous cluster formation before thermal annealing. The threshold fluence for spontaneous formation of nanoclusters in Suprasil-300 is 4×10^{16} ion/cm^2 for 1.5 MeV silver, 2×10^{17} ion/cm^2, for 2.0 MeV copper, and 2×10^{17} ion/cm^2 for 3.0 MeV gold. SRIM was used to compute the implanted ion concentration depth profile for each element at the critical fluence. These implanted ion concentration profiles were experimentally confirmed with RBS.

Heating an implanted sample increases the atomic diffusion rates by providing an activation energy to move the implanted atoms to lower energy sites in clusters, thus increasing the localized volume fraction. With an initial mean separation between implanted atoms of only a few nanometers, virtually all will diffuse locally to form clusters and will not reach the surface of the Suprasil or diffuse much deeper into it. Moreover, other experiments have shown that the initially damaged regions in the host may themselves provide favorable pathways for individual guest atoms. With additional heat treatment the near neighbor clusters may coalesce, and the host then accommodates to the metal volume distribution. RBS measurements confirm that the depth profile of the metal clusters formed after heat treatment is almost identical to, or slightly narrower than, the depth profile of the atoms initially implanted by ion bombardment [6], as shown in Figure 1.

Figure 1 shows RBS results from before and after 1200°C annealing of Suprasil substrates that were pre-implanted with a fluence of $1.2 \times 10^{17}/cm^2$ 3.6 MeV Au ions, at room temperature, indicating no significant change of the average depth distribution of Au as a result of heating.

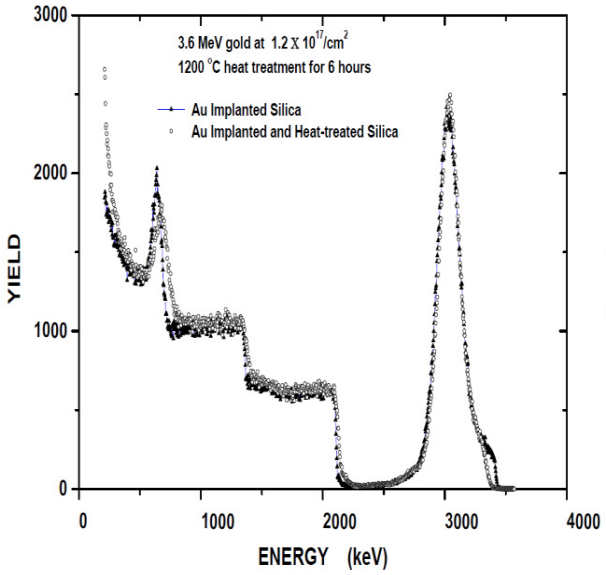

Figure 1. RBS results before and after heat treatment at 1200°C for a silica sample implanted by 3.6 MeV gold

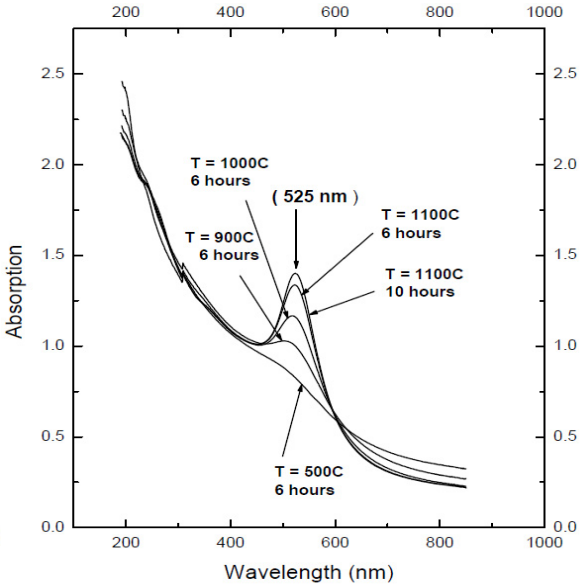

Figure 2. Optical absorption spectra from 3.6 MeV Au implanted and annealed at various temperatures

Results and data analysis

Figure 2 shows optical absorption by Suprasil substrates implanted with 3.6 MeV, $1.2 \times 10^{17}/cm^2$ Au ions, and annealed at temperatures between 500°C and 1100°C for six hours, and also one sample annealed at 1100°C for 10 hrs. This Figure shows that for an increase in the temperature, and constant thermal annealing time, the size and volume fraction of the nanocrystals increase. Similarly, for a given treatment temperature, such as 1100°C, increased thermal annealing time increases the extinction coefficient owing to increased local volume fraction and nanocrystal size.

Figure 3 shows the change in the radius of Ag nanocrystals as the heat treatment time was increased from one hour to a few days for two initial fluences of $2 \times 10^{16}/cm^2$ and $4 \times 10^{16}/cm^2$ of 1.5 MeV implanted Ag ions. As shown in this Figure, the initial radii observed before annealing are important, since the higher the fluence of implanted Ag ions in the Suprasil sample, the larger the radius of the Ag nanocrystals annealed for the same heat treatment time and temperature.

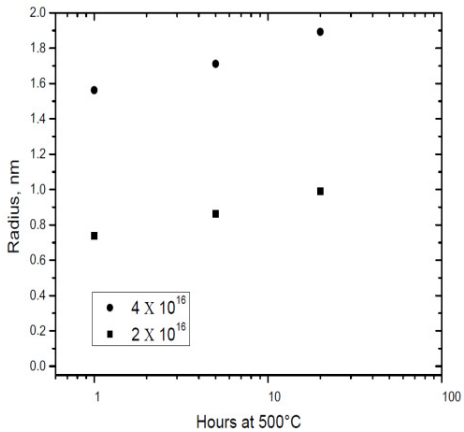

Figure 3. Radius vs. soak time at 500°C for 1.5 MeV Ag implanter Suprasil 1. Fluences are 2 x 10^{16} and 4 x $10^{16}/cm^2$

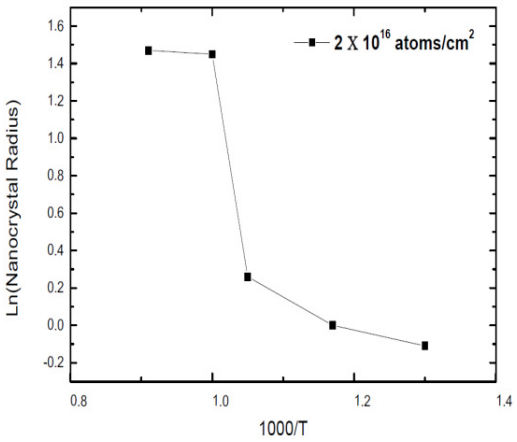

Figure 4. Natural logarithm of the radius of nanocrystals vs. 1000/heat treatment temperature for Suprasil pre-implanted by 2×10^{16}/cm^2 Au ions

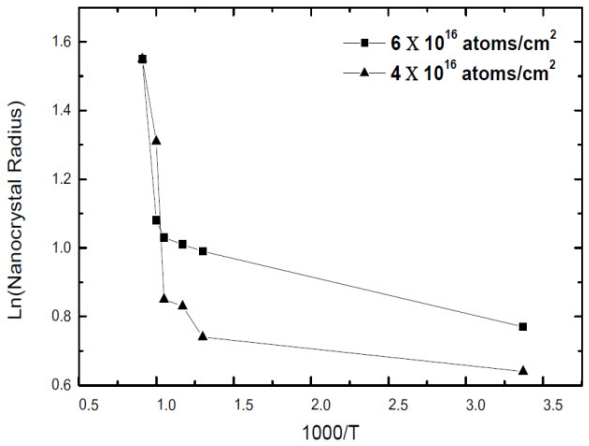

Figure 5. Natural logarithm of the radius of nanocrystals vs. 1000/heat treatment temperature, for Suprasil pre-implanted by 4 and 6×10^{16}/cm^2 Au ions.

Figures 4 and 5 show the natural logarithm of the nanocrystal radius as a function of 1000/T, where T is the heat treatment temperature, for Suprasil implanted with Au at fluences of 2×10^{16}/cm2, 4×10^{16}/cm^2, and 6×10^{16}/cm^2. As shown in these two Figures, and consistent with the data of Figure 3, the initial nanocrystal radius depends on the fluence of the implanted metal ions in Suprasil.

Figure 6 (a) shows a series of optical spectra from a single silica sample, previously implanted with gold ions, each spectrum being measured at room temperature after heat treatment for one hour at a variety of temperatures. The plasmon resonance peak is observed to narrow as the heat treatment temperature is increased. Its Full Width at Half Maximum (FWHM) is inversely related [15] to the average radius of the nanocrystals that have been formed by thermal diffusion of silver atoms in the silica (see equation 1).

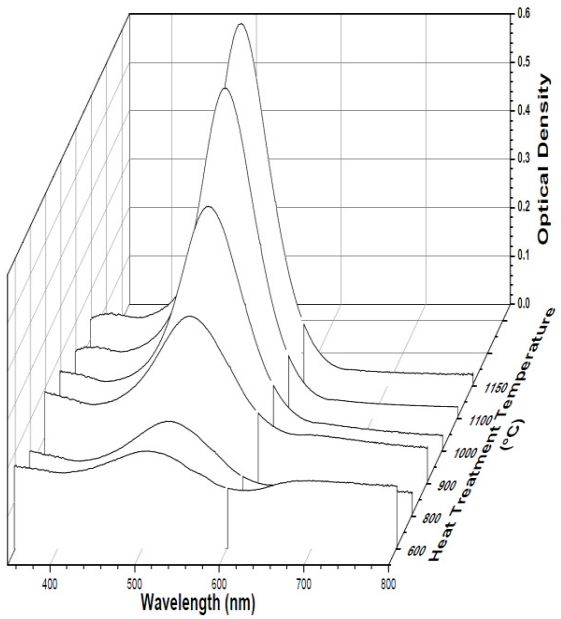

Figure 6 (a). Optical density for 2 MeV gold implanted Suprasil-1 at 2×10^{16} cm^{-2} at various heat treatment temperatures

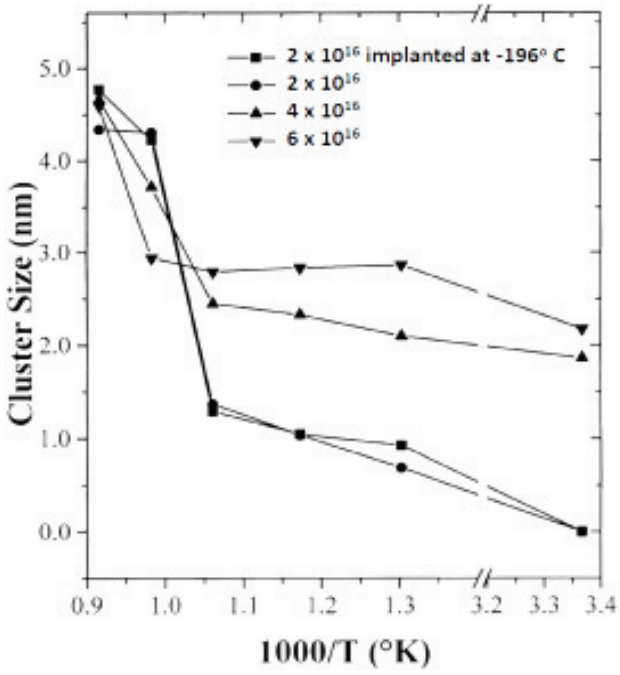

Figure 6 (b), Dependence of the cluster radius of silver as a function of the reciprocal of the heat treatment temperature for various implantation fluences.

Figure 6 (b) is a graph showing the average cluster size dependence on the reciprocal of the heat treatment temperature for three implantation fluences: 2, 4 and $6 \times 10^{16}/cm^2$ silver ions. Larger silver nanocrystals form when the implantation fluence is larger [2]. Moreover, there is a significant transition in the formation rate of large silver nanocrystals at a critical temperature corresponding to 1000/T = approx. 1.05. Evidently, important kinetics of formation of metal nanocrystals in silica samples are dominated by the dependence of the cluster size on the heat treatment temperature.

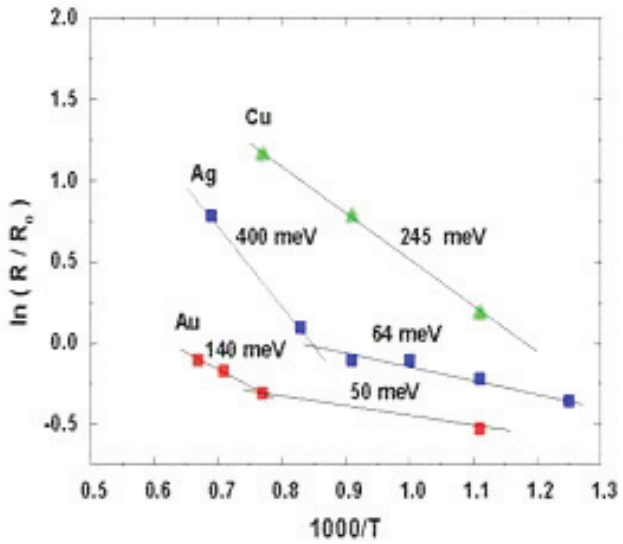

Figure 7. Observed nanocluster radii after heat treatment at temperatures T, all for 1 hour duration.

In Figure 7, we have plotted the natural logarithm of the average radius R against the inverse temperature 1000/T used for various heat treatments, each for 1 hour. Three silica samples shown were implanted with Au, Ag, and Cu ions respectively [1]. The resulting Arrhenius plot permits us to attribute activation energies E to the kinetic process of forming nanocrystals by thermal diffusion. In standard units, the graph suggests the equation

$$R / R_0 = e^{-E/kT} \quad (2)$$

The value of R_o is arbitrarily taken as 1 nm, for the determination of the energy E. However, the units of the horizontal axis of Figure 7 must be converted to meV^{-1} with a factor f = 25/0.293, using kT = 25 meV at room temperature T = 293°K.

Activation energies are shown for each estimated straight line segment in Figure 7. Although the Cu implanted sample was perhaps not treated at high enough temperatures, the Ag and Au implanted samples clearly show an abrupt change in nanocrystal formation rate at a critical heat treatment temperature.

Conclusions

Using equation 2 and Figure 7, we conclude that there is an abrupt change in the dominant activation energy for nanocrystals with radius between 1 and 3 nanometers. This is the first directly observed evidence of a dual-component mechanism for metal nanocrystal growth within silica under thermal treatment. We speculate that the faster growth rate at higher temperatures may be associated with thermal annealing of the implant-stressed host silica structure, leading to enhanced thermal diffusion of metal clusters within the surrounding silica. A further possible model for the dominance of a process with high activation at higher temperatures may be the generalized Ostwald ripening mechanism, as described in References [21,22]. This model identifies a critical average radius for developing nanocrystallites, at which point the individual mobile metal atoms needed for the ripening of larger nanocrystals at the expense of smaller ones require an extra (thermal) energy of activation in order to escape from their home lattices before migrating.

Analysis of our previously published data presents these "effective" activation energies, low for initial aggregation of random atoms, higher for the transfer of atoms from small nanocrystals to nearby larger ones. Further experimental studies are now needed, in order to determine the physical origins of these observed kinetic phenomena.

References

1. D. ILA, Z. Wu, R. L. Zimmerman, S. Sarkisov, C. C. Smith, D. B. Poker, and D. K. Hensley, *Mat. Res. Soc. Symp. Proc.* Vol. 457, 143-147 (1997)
2. D. ILA, E. K. Williams, S. Sarkisov, C. C. Smith, D. B. Poker, and D. K. Hensley, *Nucl. Inst. and Meth. in Phys. Res. B* 141, 289-291 (1998)
3. G.W. Arnold, *J. Appl. Phys.* 46 (1975) 4466.
4. G.W. Arnold, J.A. Bordes, *J. Appl. Phys.* 48 (1977) 1488.
5. D. ILA, Z. Wu, C.C. Smith, D.B. Poker, D.K. Hensley, C. Klatt, S. Kalbitzer, *Nucl. Instr. and Meth. B* 127/128 (1997) 570.
6. D. ILA, R. L. Zimmerman, C. I. Muntele, P. Thevenard, F. Orucevic, C. L. Santamaria, P. S. Guichard, S. Schiestel, G. K. Hubler, D. B. Poker, and D. K. Hensley, *Nucl. Instr. and Meth. B* 191 (2002) 416.
7. R.H. Magruder III, R.A. Zuhr, D.H. Osborne, Jr., *Nucl. Instr. and Meth. B* 99 (1995) 590.
8. Y. Takeda, T. Hioki, T. Motohiro, S. Noda, T. Kurauchi, *Nucl. Instr. and Meth. B* 91 (1994) 515.
9. D. Ila, Z. Wu, R.L. Zimmerman, S. Sarkisov, C.C. Smith, D.B. Poker, D.K. Hensley, *Mat. Res. Soc. Symp. Proc.* 457 (1997) 143.
10. C.W. White, D.S. Zhou, J.D. Budai, R.A. Zuhr, R.H. Magruder, D.H. Osborne, *Mat. Res. Soc. Symp. Proc*. 316 (1994) 449.
11. K. Fukumi, A. Chayahara, M. Adachi, K. Kadono, T. Sakaguchi, M. Miya, Y. Horino, N. Kitamura, J. Hayakawa, H. Yamashita, K. Fujii, M. Satou, *Mat. Res. Soc. Symp. Proc.* 235 (1992) 389.
12. T. van Dillen, M.L. Brongersma, E. Snoeks and A. Polman, Activation energy spectra for annealing of ion irradiation induced defects in silica glasses, *Nucl. Instr, and Methods B* 148 (1999) 221.
13. J.F. Ziegler, J.P. Biersack, U. Littmark, *The Stopping and Range of Ions in Solids*, Pergamon Press, New York, 1985. http://www.srim.org
14. D. ILA, E. K. Williams, D.B. Poker, D.K. Hensley, C. Klatt, S. Kalbitzer, *Mat. Res. Soc. Symp. Proc.* 540 (1999) 147.
15. W.T. Doyle, *Phys. Rev.* 111 (1958) 1067.
16. D. Ricard, Ph. Roussignol, Chr. Flytzanis, *Opt. Lett.* 10 (1985) 511.
17. E.R. Schineller, R.P. Flam, D.W. Wilmot, *J. Opt. Soc. Am.* 58 (1968) 1171.
18. P. D. Townsend, *Nucl. Instr. and Meth. B* 46 (1990) 18. [14), and G. Mie, *Ann. Physik* 25 (1908) 377.

19. U. Kreibig, M. Vollmer, *Optical Properties of Metal Clusters*, Springer, Berlin, 1995.
20. R.F. Haglund Jr., Quantum-dot composites for nonlinear optical applications, in: R.F. Hummel, P. Wismann (Eds.) *"Handbook of Optical Properties"* vol. II. Optics of Small Particles, Interfaces, and Surfaces, CRC Press, Boca Raton, 1997.
21. Quin-bo Wang, Finsy Robert, Hai-bo Xu and Xi Li, On the critical radius in generalized Ostwald ripening, *J. Zhejiang University Science B*, August 2005; 6(8), 705-707
22. M. B. Mohamed, Zheng L. Wang and Mostafa A. Al-Sated, Temperature-Dependent Size-Controlled Nanocluster Nucleation and Growth of Gold Nanoclusters*, J. Phys. Chem. A* 1999 103, 10255-10259